THE PHENOMENON OF STRESS INSTABILITIES IN Al-Li BINARY ALLOYS AND MICROSCOPIC MECHANISMS CONNECTED

J. Gentzbittel, G. Vigier, R. Fougeres

JOURNAL DE PHYSIQUE
Colloque C3, supplément au n°9, Tome 48, septembre 1987

THE PHENOMENON OF STRESS INSTABILITIES IN Al-Li BINARY ALLOYS AND MICROSCOPIC MECHANISMS CONNECTED

J.M. GENTZBITTEL, G. VIGIER and R. FOUGERES

Groupe d'Etudes de Métallurgie Physique et Physique des Matériaux, INSA, CNRS-UA 341, 20, Avenue Albert Einstein, F-69621 Villeurbanne Cedex, France

ABSTRACT

For several years it has been well established that aluminium alloys with lithium additions are very attractive for aerospace applications, since they offer interesting combinations of high specific strength and high specific modulus /1/,/2/. Numerous studies were carried out in order to obtain optimum mechanical properties by modifying suitably microstructures /3/,/4/,/5/. Mechanical properties are mainly dependent on interactions between dislocations and precipitates, especially δ' (Al_3Li) precipitates. Fundamental studies were carried out on Al-Li binary alloys exhibiting only δ' precipitates /6/. We have entered upon a study concerning the identification of microscopic mechanisms which control the cyclic deformation of Al-Li binary alloys. During fatigue tests, we have discovered an interesting substructure in hysteresis loops corresponding to stress instabilities in fatigue behaviour which are rigorously coupled with a strain age hardening phenomenon. The aim of this paper is to describe this phenomenon which is typical of the fatigue behaviour of Al-Li binary alloys with small δ' precipitates. In the last part of this paper, this unstable behaviour is compared to the PORTEVIN-LE CHATELIER (PLC) phenomenon. In addition, microscopic mechanism that control stress instabilities and strain age hardening are analysed in terms of interactions between dislocations and δ' precipitates.

1. EXPERIMENTAL PROCEDURE

Three polycrystalline Al-Li binary alloys, containing 0.7, 1.7 and 2.5 Wt % respectively of lithium were used for the present investigation. The 0.7 Wt % alloy was heated at 530°C for two hours then ice-water quenched and finally aged at room temperature for several months. Under these treated conditions, the 0.7 Wt % Li alloy was kept in a solid solution state as could be inferred by TEM observations and small angle X ray scattering experiments. In the case of 1.7 and 2.5 Wt % Al-Li alloys, the same solid solution treatment at high temperature, water quenching and ageing for two months at room temperature lead to an homogeneous distribution of small spherical δ' (Al_3Li) precipitates. The average diameter of δ' precipitates is approximatively equal to 1 nm. After quenching and ageing at 150°C for 5 hours, 1.7 and 2.5 Wt % Li alloys presented a coarsened δ' precipitation with an average diameter of ~15 nm. The average size of 1.7 Wt% precipitates was a little higher than that of 2.5 Wt % Li. All these results are in concordance with those reported in /7/.

Fatigue tests have been carried out in a push-pull mode, in a temperature range between room and liquid nitrogen temperatures. Cylindrical samples of 70 mm long with a diameter of 9 mm and a useful length of 40 mm were used in this study. The specimen deformation recorded using a MTS extensometer n° 632-276-23 with a measurement length of 25 mm. The cyclic deformation was controlled under total or plastic strain conditions using a specific fatigue machine having a very high displacement sensitivity /8/. Recently this testing machine was used to study interactions between crystalline defects and dislocations in the case of fatigue of pure aluminium /9/. Fatigue tests were conducted under control of a PDP 11 Digital computer with a linear time deformation dependence in the frequency range of $0.5\text{-}10^{-3}$ Hz. Most of fatigue tests were carried out at room temperature. However, some tests were performed at lower temperature in order to study the temperature dependence of the stress instability phenomenon and of the fatigue strain age hardening. Low temperature tests were performed by means of a cryogenic apparatus belonging to the fatigue machine and that was described in reference /8/.

2. EXPERIMENTAL RESULTS

2.1. The instability phenomenon

At the beginning of the fatigue process, all alloys tested presented a cyclic hardening and, after a few hundred cycles, the maximal fatigue stress remained at a constant value both in tension and compression. In the case of 2.5 Wt % alloy aged at room temperature, figure 1 shows the dependence of the maximal fatigue stress as a function of the number of cycles.

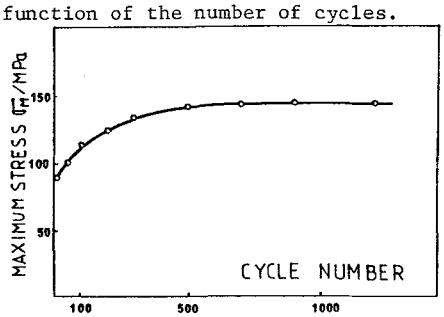

FIG. 1 - Evolution of the maximum fatigue stress versus the number of cycles. Case of the 2.5 Wt % alloy aged at room temperature. Plastic strain amplitude : $\Delta\varepsilon_p/2 = 2.10^{-3}$. Test at room temperature.

The microstructure of the cycled samples in the stabilized stress range is characterized by small δ' precipitates independently of previously ageing conditions. As a matter of fact by small angle X ray scattering experiments, it was observed a different behaviour of cycled alloys according to the temperature of ageing. For the 2.5 Wt% alloy aged at room temperature, a cycling up to the stabilized stress range leads to a slightly coarsening of δ' precipitates, their average diameter being approximatively equal to 1.5 nm. In the case of an ageing at 150°C for 5 hours (with a precipitate diameter of 15 nm) and of a cycling in the stabilized stress range, a decrease in the average diameter has been observed. It is difficult to determine if the decrement in average diameter is due to the shearing of δ' precipitates or to a new precipitation from the solid solution which can be favoured by a high vacancy production during the cyclic deformation. These two mechanisms can be probably involved during the cyclic process.

The unstable phenomenon described here in has been mainly studied in the stabilized stress range where no evolution of fatigue loops could be detected.

Figures 2 and 3 show the stabilized fatigue loop for 2.5 Wt % Li and 1.7 Wt % Li alloys respectively. These two alloys were aged at room temperature and at 150°C for two hours respectively. Then, they were cycled at a plastic strain amplitude $\Delta\varepsilon_p/2$ of 2.10^{-3}. In the plastic range of the fatigue loop, successive drops in the fatigue stress could be observed which also seemed to appear periodically. The amplitude of stress instabilities increased progressively at the beginning of the plastic range (fig. 2 and 3) up to a maximum value. This maximum value, a, and the increase of the time between two successive stress instabilities, Δt, (these two values are defined on figure 3) depended on the coupling of the fatigue machine with the physical phenomenon responsible for the unstable behaviour. Therefore, values of the instability amplitude cannot be discussed quantitatively but only in a qualitative way.

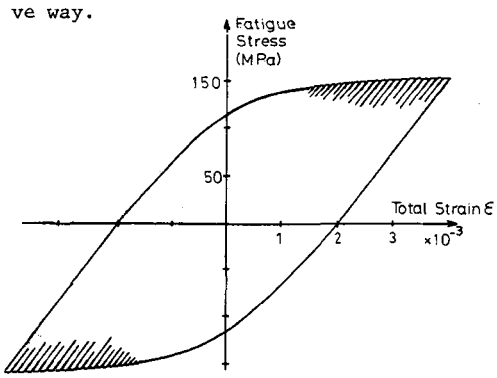

FIG. 2 - Stress instabilities in stabilized fatigue loops of the 2.5 Wt % Al-Li alloy aged two months at room temperature. Plastic strain amplitude: $\Delta\varepsilon_p/2 = 2.10^{-3}$. Test frequency : 0.01 Hz. Test conducted at room temperature.

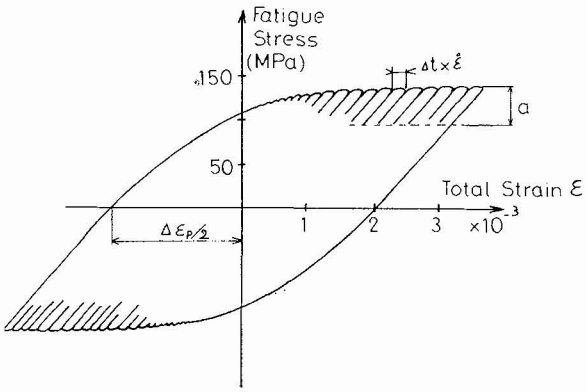

FIG. 3 - Stress instabilities in stabilized fatigue loops of the 1.7 Wt % Al-Li alloy aged five hours at 150°C. Fatigue conditions are identical to those reported in Fig.2.

2.2. Conditions for the instability phenomenon

We have noted that stress instabilities could be observed under the following experimental conditions :

1. At room temperature, the appearance of instability requires that cumulative plastic strain ε_{pc} be equal to 0.1 (ε_{pc} is given by $\varepsilon p_c = 4N(\Delta\varepsilon_p/2)$, where N is the number of cycles and $\Delta\varepsilon_p/2$ is the plastic strain amplitude) for both the 1.7 Wt % Li and 2.5 Wt % Li alloys, independently of the ageing temperature. During fatigue tests no propagation of slip bands were visible to the naked eye. On the other hand, the beginning of stress instabilities corresponds with a very strong localisation of the deformation on a single slip system in each grain of the polycrystalline specimen.

In figure 4, light micrographs show slip lines at the sample surface, obtained after different numbers of fatigue cycles. During the first fourth part of the first cycle, three different slip systems are activated in all grains. However, only one single slip line system is generally observe after several fatigue cycles ; then, the beginning of the stress instability phenomenon is characterized by the initiation of very coarse and regularly spaced slip bands. This slip band structure becomes independent of the cycle number as the stabilized stress range is reached.

The investigation of corresponding bulk microstructures by transmission electron microscopy (figure 4b) shows that there are different wholes of very fine slip lines that are perhaps in the beginning of the coarse slip band. These fine slip lines appear clearly in figure 4 although they seem to be not so marked as those described in reference /10/. Moreover, it is noticed that no coarsening effect exists on the side of the slip line and that no difference can be observed in the δ' precipitate distribution as it can be seen on dark field transmission electron micrograph.

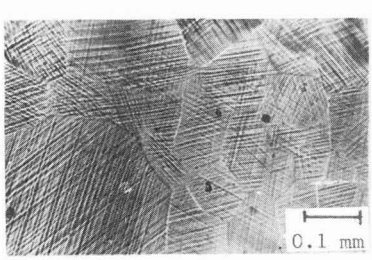

1/4 cycle

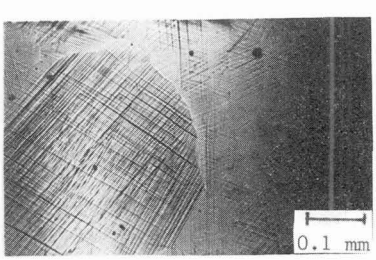

1 cycles

FIG.4a - Light micrographs of the surface sample of the 1.7 Wt % alloy aged at room temperature and cycled at different numbers of cycles with a strain amplitude $\Delta\varepsilon p/2 = 2.10^{-3}$. Note the evolution of the number of slip systems.

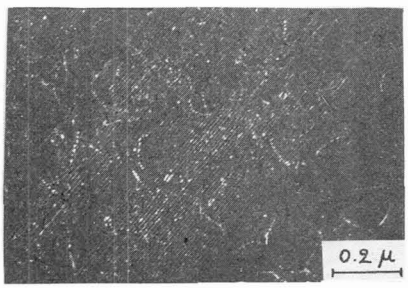

FIG 4b: T.E.M. micrograph of a fatigue sample cycled at room temperature in the stabilized stress range with a stress amplitude: $\Delta\varepsilon_p/2 = 2\times10^{-3}$.
Sample previously aged at room temperature. Test frequency: 0.0 1 Hz.

2. The amplitude value, a, of stress instabilities is strongly dependent on the test frequency (figure 5). Above a test frequency of approximatively 0.2 Hz, stress instabilities could not be detected. In a qualitative way, it can be observed, as in figure 5, that the maximum value of the parameter a is reached at a frequency of about 8.10^{-3} Hz corresponding to a plastic strain rate of $6.66.10^{-5}$ s^{-1}. Moreover, very little evolution of instabilities are observed at lower strain rates.

3. It was noticed that the stress instability phenomenon is typical of binary Al-Li alloys which form δ' precipitates. Indeed, in the case of the 0.7 Wt % Al-Li alloy with lithium atoms in a solid solution, we have never observed stress instabilities in spite of a very large range of variation of fatigue parameters (test frequency and fatigue strain amplitude).

4. On a sample prefatigued at room temperature in the stabilized stress range a decrease of the fatigue temperature leads to a diminution of the stress instability amplitude. Moreover, no stress instabilities could be observed on the 2.50 Wt % Al-Li alloy aged at room temperature, when the test temperature is lower than 0°C. In the same way, no stress instabilities could be detected on the 2.5 Wt % Al-Li alloy aged at 150°C for five hours when the fatigue test temperature is below -40°C.

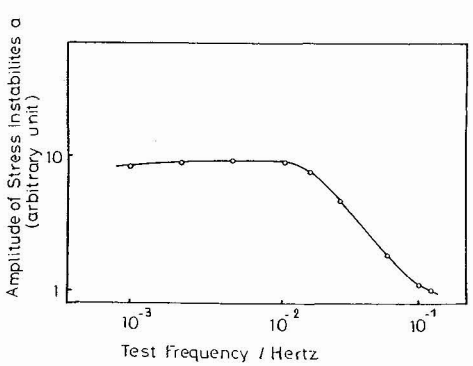

FIG. 5 - Qualitative variation of stress instability amplitude as a function of the test frequency. Case of 2.5 Wt % alloy aged two months at room temperature. Plastic strain amplitude : $\Delta\varepsilon_p=2.10^{-3}$. Test at room temperature.

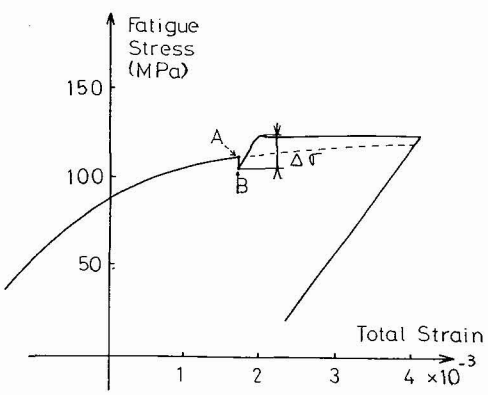

FIG. 6 - Effect of an ageing time at room temperature after stopping in the fatigue process. A stress increase Δσ is observed when the fatigue test is started again. Case of 2.5 Wt % Al-Li alloy aged at room temperature.

5. Finally, at a given test temperature for which stress instabilities exist, for instance at room temperature, if the fatigue process is arrested at a given point of the fatigue loop and the sample subsequently aged at the same temperature, an increase in stress, $\Delta\sigma$ (figure 6) could be observed when the fatigue test is started again. The small stress decrement in figure 4 from A to B, when the total strain of the sample is kept at a constant value, could be ascribed to a weak relaxation phenomenon.

After one or two further fatigue cycles, the fatigue loop becomes identical to the one obtained before the arrest of the fatigue process. It is noticed that the strain age hardening is rigorously associated with fatigue stress instabilities : no stress instabilities were seen to occur if there is no strain age hardening phenomenon.

2.3. Fatigue strain age hardening

The $\Delta\sigma$ stress increase can be quantitatively studied because the coupling with the above mentioned fatigue machine is not so important as in the case of fatigue stress instabilities.

For the same sample prefatigued in the stabilized stress range, figure 7 shows the dependence of $\Delta\sigma$, the stress increase, as a function of ageing time at room temperature after arresting the fatigue process (always at the same point of the stabilized fatigue loop). With ageing time, the stress increase, $\Delta\sigma$, is rapidly stabilized. At room temperature, $\Delta\sigma$ stabilized to a constant value after ten minutes.

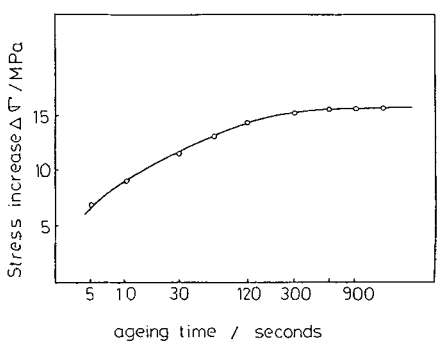

FIG. 7 : Effect of the ageing time on the value of the maximum increase stress. Case of 2.5 Wt % Al-Li alloy aged at room temperature and prealably cycled in stabilized range at a strain amplitude of 2.10^{-3}.

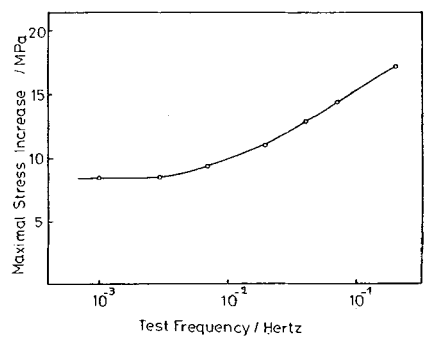

FIG. 8 - Effect of the test frequency of cycled sample on the maximum increase stress obtained by arrest of fatigue and ageing at room temperature for ten minutes.

In figure 8, the variation of the maximum value of the stress increase, $\Delta\sigma$, is shown as a function of the fatigue test frequency. As in the case of fatigue stress instabilities, the age hardening becomes stabilized at frequency values lower than 8.10^{-3} Hz.

3. DISCUSSION

When the stress instability phenomenon was observed for the first time, we naturally suspected it to becaused by some problems in testing machine. However, repeated observations and innumerable fatigue tests showed that it was not only a machine effect but also true material effect that was associated with the plastic deformation of the specimen. Under exactly same conditions of setting of testing machine, when fatigue tests were performed with a 4 Wt % Al-Cu alloy exhibiting shearable θ" precipitates, we never observed stress instabilities or strain age hardening. However, we think that conclusive evidences are given by fatigue tests in the low temperature range for which the amplitude of stress instabilities decreases as the test temperature is diminished. As a matter of fact, under these conditions, all fatigue parameters and setting conditions were kept rigorously identical.

The type of instabilities observed seems to resemble the type C of the PORTEVIN-LE CHATELIER phenomenon described in /11/. Indeed, the rough drop in the fatigue stress seems occur from a stress level that corresponds approximatively to the fatigue stress level without instabilities. However, PLC phenomenon is generally

ascribed to a dynamic interaction between dislocations and solute atoms /10/. The fact that no instabilities are detected in the 0.7 Wt % Al-Li alloy suggests that dislocation-lithium interactions are probably not involved in the observed phenomenon. Thus the stress instability seems to be associated with the δ' precipitates in the material.

In the discussion, it will be considered that small δ' precipitates are actually responsible of the stress increase $\Delta\sigma$. In order to determine the nature of the microscopic mechanism that is responsible for the stress instability, the dependence on strain age hardening (stress increase $\Delta\sigma$) with temperature and strain rate, has been investigated in the case of the 2.5 Wt % alloy aged at room temperature. The experimental procedure was the following : after an arrest of the fatigue test at a given point of the stabilized fatigue loop, obtained by cycling at room temperature and an ageing at the same temperature for ten minutes, the temperature of the sample was decreased up to a given temperature between room and liquid nitrogen temperatures. Then, at a given strain rate, the fatigue test was started again in order to determine the corresponding value of the stress increase $\Delta\sigma$. After this fatigue test at low temperature, the temperature of the sample was increased up to the room temperature and ten fatigue cycles were performed in order to obtain the previous stabilized fatigue loop.

In order to determine a new value of the stress increase, $\Delta\sigma$, corresponding to different conditions in temperature and in plastic strain rate, a new sequence of tests was then carried out from one arrest on the fatigue loop, exactly at the same point that this defined in the previously test. Different values of stress increases $\Delta\sigma$ were thus obtained with different conditions in temperature T and in plastic strain rate, $\dot{\varepsilon}$. According to the theory of the thermally activated deformation, the three variables $\dot{\varepsilon}$, T and $\Delta\sigma$ are related by the following expression : $\dot{\varepsilon} = \dot{\varepsilon}_0 \exp - \left(\frac{\Delta G}{kT}\right)$ (1), with $\dot{\varepsilon}_0$ the pre-exponential factor, k the BOLTZMANN's constant and ΔG the activation energy. According to experimental considerations, it is possible to assume that the stress increase $\Delta\sigma$ is the effective stress component, the fatigue stress σ_f (see figure 6) being considered as the internal stress. In these conditions, it immediately follows that :

$$\dot{\varepsilon} = \dot{\varepsilon}_0 \exp\left(\frac{\Delta G_0 - v s \Delta\sigma}{kT}\right) \qquad (2)$$

with ΔG_0 the total activation energy, v the activation volume, s the mean SCHMID's factor and $\sigma = \sigma_f + \Delta\sigma$. By the analysis method proposed by U.F. KOCKS and al. /12/, the profile of the thermal barrier ($s\frac{\Delta\sigma}{\mu} = f(v)$ with μ the shear modulus) has been determined.

Because the mechanism involves in the stress increase, $\Delta\sigma$, is rather insensitive to the strain rate ($m = \left.\frac{\partial \ell n\, \dot{\varepsilon}}{\partial \ell n\, \sigma}\right|_T = \simeq 20$), it has been considered /11/ that the activation volume may be given by $v \simeq kT \left.\frac{\partial \ell n\, \dot{\varepsilon}}{\partial \sigma}\right|_T$. Therefore, the barrier profile can be determined. It is reported in figure 9.

In fact, one may generally consider /12/ the variation of the activation energy ΔG with the applied stress σ to be given by :

$\Delta G = \Delta G_0 \left\{1 - \left(\frac{s\Delta\sigma}{\hat{\tau}}\right)^p\right\}^q$, where p and q are constant parameters and $\hat{\tau}$ is the resolved shear stress value at the top of the barrier corresponding to the value of $s\Delta\sigma$ at 0°K. The value of parameters p and q and of the total activation energy ΔG_0 can be identified from the experimental values of the obstacle profile reported in figure 9, the activation volume being given by $v = \partial\Delta G/\partial\sigma$. The value of p, q and ΔG_0 are equal to 1/4, 2 and 1 eV respectively. That means /11/ that the barrier profile such as that in figure 9 seems to correspond to a microscopic mechanism involving the creation of an interface step by dislocations, rather than the generation of an antiphase

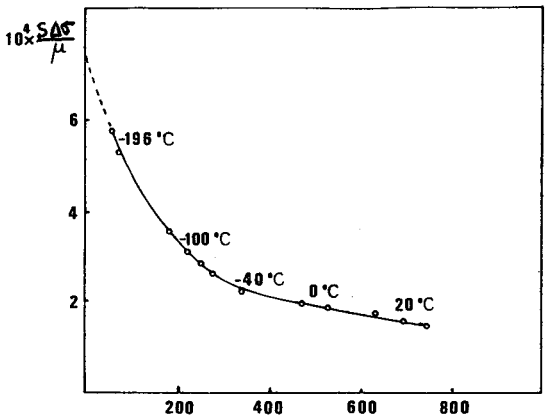

FIG. 9 - The apparent obstacle profile derived from mesuremehts of $s\Delta\sigma$ as a function of $\dot{\varepsilon}$ and T. Case of the 2.5 Wt %alloy aged at room emperature and cycled at $\Delta\varepsilon_p/2 = 2.\ 10^{-3}$ for 500 cycles. Strain age hardening for 10 mn. Variation of $s\Delta\sigma/\mu$ versus the activation volume in b^3 (b : the burgers vector of dislocations)

boundary inside the precipitate. As a matter of fact in the case of very small precipitates, it is very generally accepted that the shearing of precipitates can be controlled by the creation of an interface step /13/. For Al_3-$Li_{\delta'}$ precipitates this mechanism can be predominant if the average diameter of precipitates becomes lower than approximately 1.5 nm /6/.

In conclusion of this discussion, it appears that the fatigue strain age hardening and therefore the stress instability phenomenon seems to be related with the shearing of small δ' precipitates controlled by the creation of an interface step. Finally, the mechanical instability of the fatigue stress could be due to the instability of small δ' precipitates, as a result of successive reversions and precipitations of the δ' phase in the matrix related with the movement of dislocation. Despite of very strong arguments in favour of the interactions between dislocations and small δ' precipitates, the effect of dislocation-lithium atom interactions cannot be entierly rejected. Therefore conditions under which lithium atoms diffuse into aluminium ought to be studied in order to determine possible dynamic interactions between dislocations and lithium atoms at room temperature.

Acknowledgments : The support of this work by the research Center of CEGEDUR-PECHINEY Company in Voreppe (France) is gratefully acknowleged.

REFERENCES

/1/ B. NOBLE, S.I. HARRIS and K. DINDSDALE - J. Mater. Sci., 17, p. 461 (1982).
/2/ E.A. STARKE Jr, Th. SANDERS, I.G. PALMER - Journal of Metals, August, p. 24 (1981).
/3/ T.H. SANDERS Jr and E.A. STARKE Jr - Aluminium lithium alloy, II, ed. T.H. SANDERS Jr and E.A. STARKE Jr, Pub. Met. Soc. AIME (1983).
/4/ C. BAKER, P.J. GREGSON, S.J. HARRIS, C.J. PEEL - Aluminium lithium alloys, II, the Institute of Metals, London (1986).
/5/ P. SAINFORT, B. DUBOST and P. MEYER - M.R.S. Europe, Edition de Physique, November, p. 45 (1985).
/6/ P. SAINFORT - Thesis, Université de Grenoble (1985).
/7/ F. LIVET and D. BLOCH - Scripta Metallurgica, vol. 10, p. 1147 (1985).
/8/ J. CHICOIS - Thèse, INSA Lyon, mars (1987).
/9/ J. CHICOIS, R. FOUGERES, G. GUICHON, A. HAMEL and A. VINCENT - Acta Metallurgica, vol. 84, n° 11, p. 2157 (1986).
/10/ Y. BRECHET and al. - This congress.
/11/ J.L. STRUDEL - Dislocations et déformation plastique, Ecole d'Eté, Yravals, p. 199 (1979).
/12/ U.F. KOCKS, A.S. ARGON and M.F. ASHBY - Thermodynamics and kinetics of slip, Pergamon Press, New-York (1975).
/13/ A.J. ARDELL - Metall. Trans. A., vol. 16A, December, p. 2181 (1985).